## Experimental implementation of a versatile, below-shot-noise telecom receiver

## M.V. Jabir, N. Fajar R. Annafianto, I. A. Burenkov, A. Battou and S. V. Polyakov

National Institute of Standards and Technology, Gaithersburg, MD 20899, USA.

Joint Quantum Institute & University of Maryland, College Park, MD 20742, USA

Department of Physics, University of Maryland, College Park, MD 20742, USA.

jabirmv081@gmail.gov

**Abstract:** We demonstrate the time-resolving receiver at telecom wavelength for several encodings and alphabet lengths. We study energy-bandwidth optimisation beyond shot noise limit by enabling novel modulation scheme.

© 2022 The Author(s)

Ever-increasing data traffic over the telecom network is causing a "capacity crunch" in the underlying communication systems. Reducing the optical energy required for communication can hinder the crunch. Conventional receivers based on the classical measurement are not capable of reducing optical energy beyond the so-called shot noise limit (SNL). However, quantum measurement-enabled receivers can in principle go beyond SNL and can approach Helstrom bound, reducing the required optical energy. Energy and bandwidth are two fundamental resources needed for communication. Optimising both energy and bandwidth is equally important to enable resource efficient telecommunication. Yet, most of the experimental work in quantum receivers have been done at visible wavelength [1]. Telecom receivers have been demonstrated for short alphabets M=2 and 4, however, no telecom receiver was demonstrated beyond M=4 [2, 3]. Here we experimentally demonstrate a versatile receiver that enables different types of modulation for alphabet length  $M \ge 4$ . We studied the legacy phase shift keying (PSK), coherent frequency shift keying (CFSK), and hybrid frequency phase shift keying (HFPSK). Here we report unconditional below-the-SNL state discrimination at 1550 nm for a the above modulations (PSK, CFSK, HPFSK) and for a range of alphabet lengths,  $4 \le M \le 16$ .

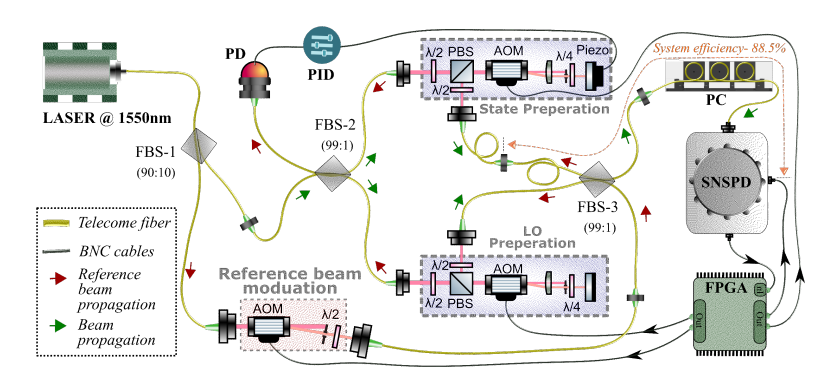


Fig. 1. The quantum telecom receiver for energy-bandwidth optimisation.

The experimental setup for quantum telecom-receiver platform is shown in Fig. 1. A fiber coupled C-band laser (at 1.55  $\mu$ m) is sent to a 90:10 fiber beam splitter-1 (FBS-1). One of the output from FBS-1 is sent to prepare the back-propagating reference beam (red arrow) for stabilizing the transmitter-receiver arrangement comprised of FBS-2 and 3 and the other part is sent to the stabilized transmitter-receiver interferometer for state discrimination. The 99:1 FBS-2 splits the beam into a input state preparation (transmitter) and a local oscillator (LO) preparation arms. LO and input state preparation modules are comprised of a acousto-optic modulator (AOM), a polarising beam splitter (PBS), two half wave plate ( $\lambda/2$ ), a quarter wave plate ( $\lambda/4$ ), a lens and a mirror. The beam passes through the AOM twice for frequency and phase modulation. The receiver is comprised of LO, FBS-3, a PC, SNSPD and FPGA. The input state and LO are combined at 99:1 FBS-3, and the output is sent to a superconducting nanowire single photon detector (SNSPD) through a polarisation controller (PC). The electronic pulse generated after each photon detection from SNSPD is sent to a field programmable gate array (FPGA) for computing the Bayesian probability [4]. The system efficiency is estimated to be 88.5(4)% which includes transmittance of both the FBS-3 and the PC and detection efficiency of SNPSD. The estimated visibility of the transmitter-receiver

interferometer is 99.4%. The reference beam intensity is modulated using the AOM with a square pulse (50% duty cycle) generated by a FPGA. During the positive pulse cycle, the reference beam is sent to the transmitter-receiver interferometer. The interferometer is stabilized via a PID controller using a conventional photodiode (PD) output as error signal. To avoid blinding the SNSPD by the back-reflected light from the reference beam, we switch the SNSPD off when stabilization occurs. During the negative pulse cycle, we switch SNSPD on and execute discrimination. Different modulation protocols are enabled by reprogramming the FPGA and no change in the physical layout is needed.

To demonstrate the quantum advantage of our telecom receiver, we have measured the symbol error rate (SER) for PSK, CFSK, and HFPSK modulations and M=4, 8, and 16. Because M=16 is the most challenging experimental case, here we show results for all the above modulations and  $M = M_f \times M_{ph} = 16$  at 1.5 photons per bit only. In Fig. 2 (a) we plot symbol error rate (SER) vs. the number of phases used per one carrier frequency  $M_{ph}$ = 1 to 16, so that  $M_f = 16/M_{ph}$ . CFSK and PSK are limiting cases of HFPSK when  $M_{ph} = 1$  and  $M_f = 1$ , respectively. For comparison, we plot absolute and and adjusted SNLs for our system efficiency. As it is evident from the figure, all the experimental points are unconditionally below the SNL. The quantum advantages are shown in decibel (dB) near each experimental results. The maximum advantage is achieved for the CFSK for 1.5 photons per bit because CFSK benefits the most from time-resolved receivers. Note here that this work is the first experimental demonstration of below-the-SNL telecom receivers for long (M = 16) alphabets.

We also study energy-bandwidth optimisation in quantum enabled communication links. We plot energy consumption (photons per bit) versus spectral efficiency (bits/s/Hz) at SER=15% in Fig. 2 (b). The result shows that CFSK has lowest energy consumption for the same error rate compared to the other modulations, but it reduces spectral efficiency. But,  $M_f \times M_{ph}$ =8×2-HFPSK can increase the spectral efficiency nearly by the factor of two without increasing energy consumption in comparison to 16-CFSK. In contrast, the energy consumption of PSK modulation rapidly grows with M even when a quantum telecom receiver is used. Interestingly, this rapid growth can be significantly reduced with a small expansion into the bandwidth by using  $M_f \times M_{ph}$ =2×8-HFPSK, which reduce 70% of energy consumption compared to 16-PSK at the expense of 30% reduction in spectral efficiency.

In conclusion, we demonstrate the time-resolving telecom receiver for alphabet length M > 4 for different modulations and its versatility. We investigate the energy consumption and spectral efficiency of multiple modulation protocols to obtain experimental resource optimization limits in a quantum-enabled communication channel. We have shown experimentally the unconditional quantum advantage of our receiver for all studied modulation protocols including legacy (PSK) and quantum-inspired protocols (CFSK, HPFSK). This work enables below-the-SNL telecom receivers for larger alphabets, here M=8, 16.

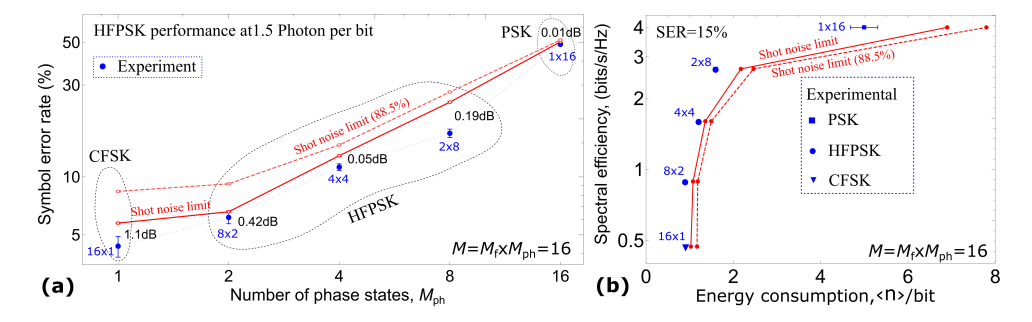


Fig. 2. (a) Quantum advantage of our telecom receiver for different modulations. (b) Energy consumption vs. Spectral efficiency. Solid red lines: absolute SNL. Dotted red lines: SNL adjusted for our system efficiency (88.5(4)%). Blue dots: experimental results.

## References

- I. A. Burenkov, M. V. Jabir, and S. V. Polyakov, "Practical quantum-enhanced receivers for classical communication," AVS Quantum Sci. 3, 025301 (2021).
- 2. M. L. Shcherbatenko, M. S. Elezov, G. N. Goltsman, and D. V. Sych, "Sub-shot-noise-limited fiber-optic quantum receiver," Phys. Rev. A 101, 032306 (2020).
- 3. S. Izumi, J. S. Neergaard-Nielsen, S. Miki, H. Terai, and U. L. Andersen, "Experimental demonstration of a quantum receiver beating the standard quantum limit at telecom wavelength," Phys. Rev. Appl. 13, 054015 (2020).
- 4. I. A. Burenkov, M. V. Jabir, A. Battou, and S. V. Polyakov, "Time-resolving quantum measurement enables energy-efficient, large-alphabet communication," PRX Quantum 1, 010308 (2020).